Inverse modeling of European CH 4 emissions 2001–2006

P. Bergamaschi, M. Krol, J. Meirink, F. Dentener, A. Segers, J. van Aardenne, S. Monni, A. Vermeulen, M. Schmidt, M. Ramonet, et al.

Inverse modeling of European CH_4 emissions 2001–2006

P. Bergamaschi,[1] M. Krol,[2,3,4] J. F. Meirink,[5] F. Dentener,[1] A. Segers,[1] J. van Aardenne,[1,6] S. Monni,[1] A. T. Vermeulen,[7] M. Schmidt,[8] M. Ramonet,[8] C. Yver,[8] F. Meinhardt,[9] E. G. Nisbet,[10] R. E. Fisher,[10] S. O'Doherty,[11] and E. J. Dlugokencky[12]

Received 12 March 2010; revised 20 July 2010; accepted 20 August 2010; published 30 November 2010.

[1] European CH_4 emissions are estimated for the period 2001–2006 using a four-dimensional variational (4DVAR) inverse modeling system, based on the atmospheric zoom model TM5. Continuous observations are used from various European monitoring stations, complemented by European and global flask samples from the NOAA/ESRL network. The available observations mainly provide information on the emissions from northwest Europe (NWE), including the UK, Ireland, the BENELUX countries, France and Germany. The inverse modeling estimates for the total anthropogenic emissions from NWE are 21% higher compared to the EDGARv4.0 emission inventory and 40% higher than values reported to U.N. Framework Convention on Climate Change. Assuming overall uncertainties on the order of 30% for both bottom-up and top-down estimates, all three estimates can be still considered to be consistent with each other. However, the uncertainties in the uncertainty estimates prevent us from verifying (or falsifying) the bottom-up inventories in a strict sense. Sensitivity studies show some dependence of the derived spatial emission patterns on the set of atmospheric monitoring stations used, but the total emissions for the NWE countries appear to be relatively robust. While the standard inversions include a priori information on the spatial and temporal emission patterns from bottom-up inventories, a further sensitivity inversion without this a priori information results in very similar NWE country totals, demonstrating that the available observations provide significant constraints on the emissions from the NWE countries independent from bottom-up inventories.

Citation: Bergamaschi, P., et al. (2010), Inverse modeling of European CH_4 emissions 2001–2006, *J. Geophys. Res.*, *115*, D22309, doi:10.1029/2010JD014180.

1. Introduction

[2] The atmospheric mixing ratios of the major anthropogenic greenhouse gases (GHGs) CO_2, CH_4, and N_2O have increased considerably since pre-industrial times [*Forster et al.*, 2007]. General concern about the impact of these increasing mixing ratios on the Earth's radiative balance has lead to the United Nations Framework Convention on Climate Change (UNFCCC), which requires signatory countries to report their annual GHG emissions of CO_2, CH_4, N_2O, perfluorocarbons (PFCs), hydrofluorocarbons (HFCs), and SF_6. Linked to the UNFCCC, the Kyoto protocol entered into force in 2005, setting legally binding emission reduction targets for the Annex-1 parties by 2008–2012. Reporting under these international agreements is so far entirely based on bottom-up inventories, using statistical data and emission factors [*Intergovernmental Panel on Climate Change* (*IPCC*), 1996]. While bottom-up estimates of fossil CO_2 emissions are generally assumed to be relatively accurate, considerable uncertainties exist especially for CH_4 and N_2O, mainly due to the large variability of emission factors for major source categories.

[3] Complementary to bottom-up emission inventories, inverse modeling can provide top-down emission estimates, tracing back measured atmospheric mixing ratios to the regions where GHGs were emitted, providing a means to verify bottom-up inventories [*Bergamaschi*, 2007; *Manning*

[1]Institute for Environment and Sustainability, European Commission Joint Research Centre, Ispra, Italy.
[2]SRON Netherlands Institute for Space Research, Utrecht, Netherlands.
[3]Wageningen University and Research Centre, Wageningen, Netherlands.
[4]Institute for Marine and Atmospheric Research Utrecht, Utrecht, Netherlands.
[5]Climate and Seismology Department, Royal Netherlands Meteorological Institute, De Bilt, Netherlands.
[6]Now at Air and Climate Change Programme, European Environment Agency, Copenhagen, Denmark.
[7]Department of Biomass, Coal and Environment, Energy Research Centre of the Netherlands, Petten, Netherlands.
[8]Laboratoire des Sciences du Climat et de l'Environment, Gif sur Yvette, France.
[9]Umweltbundesamt, Messstelle Schauinsland, Kirchzarten, Germany.
[10]Department of Earth Sciences, Royal Holloway, University of London, Egham, UK.
[11]School of Chemistry, University of Bristol, Bristol, UK.
[12]Global Monitoring Division, Earth System Research Laboratory, NOAA, Boulder, Colorado, USA.

0148-0227/10/2010JD014180

et al., 2003]. The need for independent verification has also been recognized by IPCC [*IPCC*, 2000], and is also likely to play an important role in post-Kyoto agreements which are currently under negotiation [*Committee on Methods for Estimating Greenhouse Gas Emissions*, 2010]. In recent years, increasing efforts have been made to use inverse modeling on the regional scale as first steps toward independent verification. The central prerequisite for such regional inversions is the availability of regional GHG measurements (ideally quasi-continuous measurements) which are sensitive to regional emissions and high-resolution inverse models. Several regional inverse modeling studies applied Lagrangian particle dispersion models (LPDMs), for example, for estimates of CH_4 and N_2O emissions from Europe [*Manning et al.*, 2003], United States and Canada [*Kort et al.*, 2008], and California [*Zhao et al.*, 2009]. In addition, also model-independent methods based on tracer correlations (e.g., using ^{222}Rn) have been used for regional top-down estimates [*Levin et al.*, 1999; *Messager et al.*, 2008; *Wunch et al.*, 2009]. While LPDMs usually provide high spatial resolution, they are mostly run at limited domains in space and time, and therefore require the reconstruction of global background mixing ratios either from global models or observations (which is also the case for model-independent methods). *Bergamaschi et al.* [2005] presented estimates of European CH_4 emissions based on the TM5 model [*Krol et al.*, 2005], a two-way nested Eulerian zoom model. The zooming allows relatively high resolution simulations (1° × 1°) over the region of interest at reasonable CPU costs, while nesting into the global domain (run at 6° × 4° resolution) ensures that simulated global background fields are consistent with global background observations. *Bergamaschi et al.* [2005] employed the so-called synthesis inversion technique, optimizing emissions from predefined European and global regions. Although this study used a relatively large number of regions (for Europe separate regions were chosen for major countries or clusters of smaller countries), this technique generally bears the risk of being affected by aggregation error [*Kaminski et al.*, 2001], since the spatial emission patterns within the predefined regions cannot be further optimized in the inversion. Recently, a four-dimensional variational (4DVAR) technique has been developed and implemented for the TM5 model [*Bergamaschi et al.*, 2009; *Meirink et al.*, 2008], which allows emissions to be optimized at the model grid cell scale, hence minimizing the aggregation error. In this paper we present updated estimates of European emissions based on the new TM5–4DVAR inverse modeling system.

[4] *Bergamaschi et al.* [2009] demonstrated that satellite data (such as from the SCIAMACHY instrument onboard the European Research Satellite ENVISAT) can provide valuable complementary information in particular in tropical regions which are poorly monitored by surface observations. However, the accuracy of surface measurements is generally much higher than current satellite measurements, and in particular continuous surface measurements (e.g., with hourly or better time resolution) can provide significant constraints on the regional emissions. In the present study we apply only such surface measurements from European monitoring sites, complemented by flask samples from the global NOAA/ESRL network.

[5] The specific objectives of the present study are (1) to compare the new European CH_4 emission estimates with the previous synthesis inversion for year 2001, (2) to extend the analysis to the period 2001–2006 using various additional European observations which became available in the meantime, and (3) to analyze in detail the sensitivity of the derived emissions especially with respect to model settings, applied a priori bottom-up inventories and observational data used in the inversion. The extension of the analysis to the 2001–2006 period in this study mainly serves to investigate the robustness of the derived emissions, rather than providing an analysis of emission trends (which are assumed to be relatively small over this period).

2. Measurements

2.1. Monitoring Stations

[6] The European monitoring stations used in the inversions are compiled in Table 1. They include sites with quasi-continuous measurements (i.e., providing data with hourly or better time resolution) from various monitoring networks or research groups: the operational network of the German Umweltbundesamt (UBA), the French RAMCES (Réseau Atmosphérique de Mesure des Composés à Effet de Serre) network (including also some sites with weekly flask sampling) [*Schmidt et al.*, 2006], the AGAGE (Advanced Global Atmospheric Gases Experiment) network [*Cunnold et al.*, 2002; *Rigby et al.*, 2008], Energy research Centre of the Netherlands (ECN), the National Institute for Public Health and the Environment (RIVM), and Royal Holloway University of London (RHUL). Furthermore, European and global flask measurements are used from the NOAA Earth System Research Laboratory (ESRL) global cooperative air sampling network [*Dlugokencky et al.*, 2003, 2009] (The global monitoring sites used in this study are compiled in the auxiliary material (Table S1).)[1] We generally apply the NOAA04 CH_4 standard scale in this study [*Dlugokencky et al.*, 2005]. CH_4 measurements from NOAA, UBA, ECN, and RHUL were already reported on this scale. The RAMCES data were provided on the previous NOAA CMDL83 scale and converted to the NOAA04 scale using the scaling factor 1.0124 [*Dlugokencky et al.*, 2005]. CH_4 data from the AGAGE network were converted using a scaling factor of 1.0003 [*Prinn et al.*, 2000]. To check the consistency of this scaling, the continuous AGAGE data from Mace Head were compared with NOAA flask samples at this site, resulting in annual mean biases smaller than 1.7 ppb (yearly average of bias for measurements coinciding within 1 h) during the period 2001–2006. For the UBA station Schauinsland, the continuous measurements were compared with independent flask samples analyzed by the university Heidelberg, showing annual mean biases smaller than 1.3 ppb. Furthermore, comparison performed in the frame of the European projects MethMoniteur, IMECC and Geomon showed that the CH_4 measurements of the RAMCES, NOAA, UBA, ECN and RHUL networks agreed within 3 ppb.

[7] Figure 1 displays the temporal coverage of the observational data for the set of stations used in our refer-

[1] Auxiliary materials are available in the HTML. doi:10.1029/2010JD014180.

Table 1. European Monitoring Stations Used in the Inversions[a]

Identification	Station Name	Data Source	Latitude (deg)	Longitude (deg)	Altitude (m asl)	ST	DS	EU01	EU02	EU03	EU04	EU05
STM	Ocean station M, Norway	NOAA[b]	66.00	2.00	5	FM		x	x	x	x	x
ICE	Heimay, Vestmannaeyjar, Iceland	NOAA[b]	63.34	−20.29	127	FM		x	x	x	x	x
BAL	Baltic Sea, Poland	NOAA[b]	55.35	17.22	28	FM		x	x	x	x	x
ZGT	Zingst, Germany	UBA[b]	54.44	12.72	1	CM	DY				x	
KMW	Kollumerwaard, Netherlands	RIVM[c]	53.33	6.28	0	CM	DY				x	
MHD	Mace Head, Ireland	AGAGE[d]	53.33	−9.90	25	CM	DY	x	x	x	x	x
CB4	Cabauw tall tower, Netherlands	ECN[b]	51.97	4.93	198	CM	DY	x	x	x	x	x
LON	Royal Holloway University, London, UK	RHUL[b]	51.43	−0.56	45	CM	DY	x		x		
DEU	Deusselbach, Germany	UBA[b]	49.76	7.05	480	CM	DY				x	
GIF	Gif sur Yvette, France	RAMCES[e]	48.72	2.15	20	CM	DY	x		x	x	
SIL	Schauinsland, Germany	UBA[b]	47.91	7.91	1205	CM	NI	x	x		x	x
ZUG	Zugspitze, Germany	UBA[b]	47.42	10.98	2960	CM	NI				x	x
HUN	Hegyhatsal, Hungary	NOAA[b]	46.95	16.65	344	FM		x	x	x	x	x
PUY	Puy de Dome, France	RAMCES[e]	45.77	2.97	1465	FM		x	x	x		
BSC	Black Sea, Constanta, Romania	NOAA[b]	44.17	28.68	3	FM		x	x	x	x	x
PDM	Pic du Midi, France	RAMCES[e]	42.94	0.14	2877	FM		x	x	x		
BGU	Begur, Spain	RAMCES[e]	41.97	3.23	13	FM		x	x	x		

[a]The column 'ST' indicates the sampling type (FM, flask measurements; CM, continuous measurements), and the column 'DS' is the diurnal sampling of continuous measurements (DY, during daytime; NI, during nighttime). Columns EU01−EU05 indicate which stations (marked by x) were used in the different networks applied in various sensitivity experiments (see Table 3). In addition, global monitoring sites are used to constrain the global background mixing ratios (see auxiliary material Table S1).
[b]NOAA04 scale.
[c]Converted to NOAA04 using scaling factor 0.9973.
[d]Converted to NOAA04 using scaling factor 1.0003.
[e]CMDL83 scale converted to NOAA04 using scaling factor 1.0124.

ence inversion (see section 3.4) over the time period 2001–2006. As described in section 3.2, at most one observation per day is taken from the quasi-continuous observations. Figure 1 illustrates that, apart from some short gaps, the data coverage is overall relatively continuous over our analysis period.

2.2. Aircraft Profiles Used for Validation

[8] For validation of simulated CH_4 mixing ratios measurements of aircraft profile samples were used from 3 European sites in Scotland, France and Hungary (Table 2), operated within the European CarboEurope project. The analyses of these samples were performed at LSCE, with the same protocols used as for the RAMCES surface measurements. The aircraft data were not used in the inversions and serve to validate the vertical gradient of simulated mixing ratios between the surface and ~3 km altitude.

3. Modeling

3.1. TM5-4DVAR Inverse Modeling System

[9] We employ the TM5-4DVAR inverse modeling system. Essential parts of the system are described in detail by *Meirink et al.* [2008] and subsequent further developments by *Bergamaschi et al.* [2009]. The optimal set of model parameters (state vector $\boldsymbol{x}$) is obtained by iteratively minimizing the cost function,

$$J(\boldsymbol{x}) = \frac{1}{2}(\boldsymbol{x}-\boldsymbol{x}_B)^{\mathrm{T}}\mathbf{B}^{-1}(\boldsymbol{x}-\boldsymbol{x}_B) + \frac{1}{2}\sum_{i=1}^{n}(H_i(\boldsymbol{x})-\boldsymbol{y}_i)^{\mathrm{T}}\mathbf{R_i}^{-1}(H_i(\boldsymbol{x})-\boldsymbol{y}_i), \quad (1)$$

where $\boldsymbol{x}_B$ is the a priori estimate of $\boldsymbol{x}$, and $\mathbf{B}$ the parameter error covariance matrix (containing the uncertainties of the parameters and their correlations in space and time). Here $\boldsymbol{y}$ denotes the set of observational data, $\mathbf{R}$ their corresponding error covariance matrix, and $H(\boldsymbol{x})$ the model simulations corresponding to the observations. The assimilation is discretized into assimilation time slots of 3 h, denoted by index i in equation (1). Observations and model values are averaged over this interval.

[10] The minimization of the cost function J requires the evaluation of the gradient of J with respect to the state vector,

$$\nabla J(\boldsymbol{x}) = \mathbf{B}^{-1}(\boldsymbol{x}-\boldsymbol{x}_B) + \sum_{i=1}^{n}\mathbf{H_i^T}\mathbf{R_i}^{-1}(H_i(\boldsymbol{x})-\boldsymbol{y}_i), \quad (2)$$

where $\mathbf{H^T}$ is the adjoint of the tangent linear model operator [*Bergamaschi et al.*, 2009; *Krol et al.*, 2008; *Meirink et al.*, 2008].

[11] As in the study of *Bergamaschi et al.* [2009], we apply a 'semiexponential' description of the probability density function (PDF) for the a priori emissions to enforce that a posteriori emissions remain positive,

$$\begin{aligned} e &= e_{apri\,0}\,\exp(x) \quad for\ x<0 \\ e &= e_{apri\,0}(1+x) \quad for\ x>0 \end{aligned}, \quad (3)$$

where the a priori emissions e_{apri0} are used as a constant (per grid cell, emission group, and month), and the emission parameter x is optimized instead. Here x is set a priori to zero, and assumed to have a Gaussian PDF. The use of this 'semiexponential' PDF results in small differences in the calculated country totals compared to a Gaussian PDF for the a priori emissions, but the differences (~2% for NWE total emissions) are small compared to the overall model uncertainties estimated to be ~30% (see section 4.1).

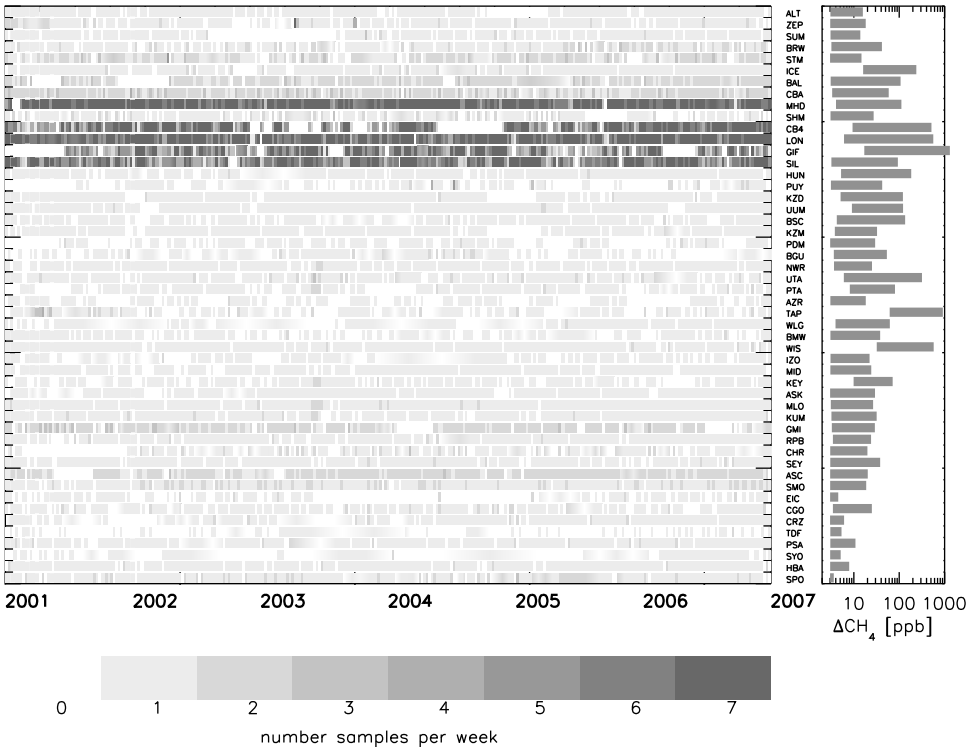

Figure 1. (left) Coverage of observational data from the different monitoring stations used in the reference inversion S1 over the period 2001–2006. (right) Range of calculated overall data uncertainties according to equation (4) (for most stations largely due to the model representativeness error).

[12] To minimize the cost function, the m1qn3 algorithm [*Gilbert and Lemaréchal*, 1989] is applied, which appeared to be more efficient for nonlinear model operators $H(\boldsymbol{x})$ than the outer/inner loop system used by *Bergamaschi et al.* [2009].

[13] Our 4DVAR system is based on the two-way nested atmospheric zoom model TM5 [*Krol et al.*, 2005]. In this study we apply the zooming with 1° × 1° resolution over Europe, while the global domain is simulated at a horizontal resolution of 6° × 4°. TM5 is an offline transport model, driven by meteorological fields (using 03–12 h forecasts) from the European Centre for Medium-Range Weather Forecasts (ECMWF) Integrated Forecast System (IFS) model. For the present study we apply the ERA-INTERIM meteorological fields, a reanalysis of the period from 1989 until present, to ensure consistent meteorological fields over the time period analyzed (2001–2006). We employ the standard TM5 version (TM5 cycle 1), with 25 vertical layers, defined as a subset of the 60 layers used in the ECMWF IFS model operationally until 2006 and for the ERA-INTERIM reanalysis.

3.2. Model Representativeness Error

[14] An important component in the set up of the inversion is the specification of realistic uncertainties for the observational data, which includes both the measurement uncertainty (which is usually relatively well defined) and the less well characterized capability of the model to represent these measurements. To better quantify the model representativeness error (sometimes also referred to as 'model-data mismatch error'), we developed a new scheme that evaluates the sensitivity of the simulated mixing ratios at a station to the emissions in the local grid cell. This serves to estimate the uncertainty that arises because in the model the emissions are mixed instantaneously over the whole grid cell. In reality the mixing ratio monitored by a station depends on the subgrid-scale variability of the emissions and the prevailing wind direction. For instance, depending on the location of the emissions relative to the monitoring station and the prevailing wind direction, these local emissions might not be detected in the real observations, if they are downwind of the station. On the other hand, if the real emissions are located upwind of the station, these emissions may lead to a larger signal than simulated in the model in which the emissions have been mixed over the entire grid cell.

[15] To estimate the impact of these local emissions, a new scheme has been implemented based on the following simplifying assumptions: (1) the tracer mass emitted from the local grid cell during each model time step is assumed to be mixed instantaneously within the boundary layer (using the TM5 boundary layer height based on the ECMWF analyses), (2) in case of increasing boundary layer height

Table 2. CarboEurope Aircraft Profiles Used for Validation[a]

Identification	Site Name	Data Source	Latitude (deg)	Longitude (deg)	ST
GRI	Griffin, UK	RAMCES[b]	56.55	−2.98	FM
ORL	Orleans, France	RAMCES[b]	47.83	2.50	FM
HNG	Hungary	RAMCES[b]	46.95	16.65	FM

[a]The aircraft data are based on flask measurements (FM).
[b]CMDL83 scale converted to NOAA04 using scaling factor 1.0124.

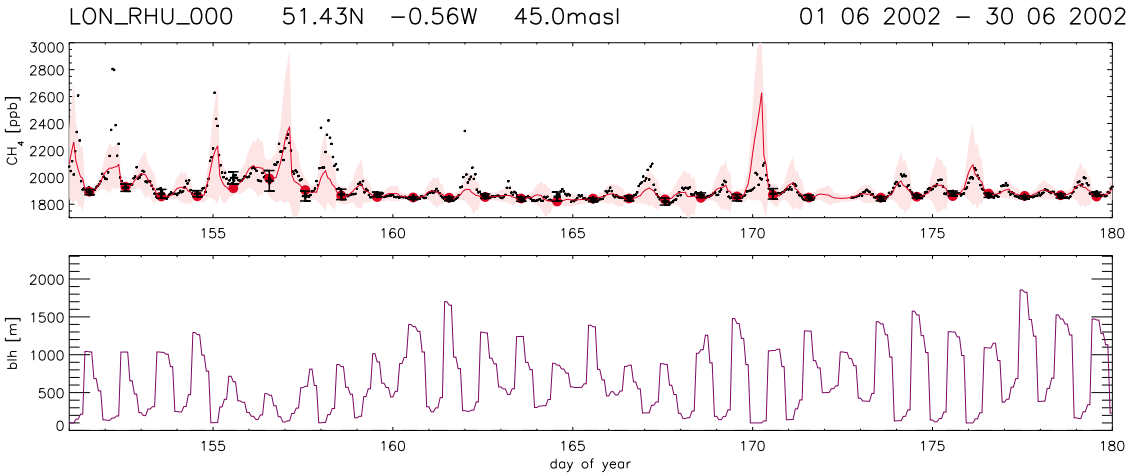

Figure 2. Illustration of model representativeness error and sampling strategy. (top) Observed (black dots: hourly values) and simulated mixing ratios (red line: a posteriori simulation) for London (June 2002). The light-red shaded area indicates the model representativeness error, which is typically large during night, when mixing ratios are enhanced due to the enrichment of local sources in the shallow nocturnal boundary layer. The solid red circles are the a posteriori model values representing the 3 h average during daytime (1200–1500 local time), and the black symbols with error bars the corresponding 3 h average of observations and the applied overall data uncertainty Δy_{tot} (according to equation (4)). (bottom) Boundary layer height in the TM5 model.

(relative to the previous time step), the tracer mass from the local emissions is mixed over the increasing mixing volume, which leads to decreasing mixing ratios, and (3) in case of decreasing boundary layer height the tracer mass above the boundary layer is released to the free troposphere (or residual layer), and is not considered anymore in subsequent time steps. The integration time for evaluation of this scheme is determined by the turnover time of the grid cell air mass. This time scale is estimated from the horizontal advection of masses, but is set to a maximum of 3 days. This scheme is only applied when the monitoring station is below the model boundary layer top height. The impact of the local emissions on simulated mixing ratios at the monitoring station calculated by this scheme is used as estimate for the uncertainty arising from the subgrid-scale variability of the emissions and is denoted Δy_{BL} (see equation (4)).

[16] In addition, we generally also evaluate the 3D gradient of simulated mixing ratios to the neighboring grid cells [*Bergamaschi et al.*, 2005; *Rödenbeck et al.*, 2003], to account for potential model errors in case of large gradients (due to subgrid-scale variability of the exchange of air masses between neighboring grid cells or due to errors in the numerical treatment of advection). Furthermore, consideration of the gradient to lower (if existing) and upper grid cell neighbors provides an estimate for potential errors due to the vertical sampling position of the station in the model, i.e., related to a potential misrepresentation of the altitude of the station within the frame of the model averaged orography.

[17] The overall data uncertainty Δy_{tot} is then estimated as

$$\Delta y_{tot} = \left[\Delta y_{BL}^2 + \Delta y_{3D}^2 + \Delta y_t^2 + \Delta y_{OBS}^2\right]^{1/2}, \qquad (4)$$

where Δy_{BL} is the uncertainty estimate for stations in the boundary layer described above, Δy_{3D} the 3D gradient to the neighboring grid cells, Δy_t the standard deviation of mixing ratios within the 3 h assimilation time slot (the maximum of the standard deviations of the model simulations and the observations), and Δy_{OBS} the measurement uncertainty, which was set to 3 ppb.

[18] The Δy_{tot} values exhibit large differences among the stations (see right panel of Figure 1), and for many stations also a large temporal variation, as illustrated for London in Figure 2. For this station (as for most stations in the continental boundary layer) Δy_{BL} is the dominant term for Δy_{tot}. During night, Δy_{tot} increases significantly, in parallel with increasing mixing ratios, and Δy_{tot} is typically of the same order of magnitude as the nocturnal increase of mixing ratios, which demonstrates the consistency of our Δy_{tot} estimates, since this increase of mixing ratios is mainly due to the emissions of the local grid cell trapped below the nocturnal boundary layer.

[19] For the assimilation of quasi-continuous observations generally only 1 value per day is used to avoid an overconstraining of the inversion: subsequent hourly measurements are usually correlated in time, while we use the assumption that the measurements are uncorrelated (**R** in equation (1) is diagonal). Stations in the boundary layer are sampled during daytime (average 1200–1500 local time), when measurements (and model simulations) are usually representative of large regions and much less affected by local emissions. In contrast, mountain stations are sampled during nighttime (0000–0300 local time) to avoid the potential influence of upslope transport on the measurements, which is frequently observed at mountain stations during daytime and which cannot be simulated correctly by a relatively coarse-scale atmospheric model.

3.3. Inversion Setup

[20] The Emission Database for Global Atmospheric Research (EDGARv4.0) is used as a priori estimate of the anthropogenic CH_4 emissions (S. Monni et al., manuscript in preparation, 2010). We apply a priori constant emissions

throughout the year for all anthropogenic emissions except rice paddies, for which the seasonal variation from *Matthews et al.* [1991] is applied to the EDGARv4.0 inventory, and biomass burning, for which the GFED v2 inventory [*van der Werf et al.*, 2004] is used. For natural sources, we employ the same emission inventories as described by *Bergamaschi et al.* [2009]. In the inversion, 4 groups of emissions are optimized independently: (1) wetlands, (2) rice, (3) biomass burning, and (4) all remaining source categories. This approach separates the first 3 categories with large seasonal cycles from the remaining sources, which are assumed to be relatively constant throughout the year. The remaining sources were grouped together, since further differentiation of the individual source categories in the inversion would require a clear spatial separation of their emissions and good a priori knowledge of their spatial distribution. The temporal correlations [*Meirink et al.*, 2008] for the first 3 categories are set to zero and for the remaining sources to 9.5 months (corresponding to a month-to-month correlation coefficient of 0.9). The uncertainties of emissions are set to 100% of a priori emissions (per grid cell and month) for each of the 4 emission groups.

[21] For northwest Europe, which is the major focus of this study, mainly the 'remaining sources' are relevant, including major anthropogenic emissions from ruminants, landfills, and energy production and use (coal, oil and natural gas). Since this source group also includes some minor natural sources and the soil sink, the optimized emissions are redistributed to the individual categories using their partitioning (per grid cell and month) in the a priori inventories. This procedure serves to separate the natural emissions from the derived total emissions, to allow a consistent comparison with UNFCCC numbers. National total emissions are calculated from the gridded model emissions (on $1° \times 1°$ resolution) by overlaying the country masks from the EDGARv4.0 database. In addition, offshore emissions (oil and gas production in the North Sea) are added to the corresponding countries according to the EDGARv4.0 database. The sampling of national total emissions from the gridded emissions inevitably leads to small errors since some grid cells are shared by different countries. Comparison with the original values for the country totals from the EDGARv4.0 database, however, showed that this error is generally below 1.5% for the countries (or groups of countries) discussed in this study.

[22] Chemical destruction of CH_4 by OH radicals in the troposphere is simulated using precalculated monthly OH fields based on Carbon Bond Mechanism 4 (CBM-4) chemistry and optimized with methyl chloroform [*Bergamaschi et al.*, 2005; *Houweling et al.*, 1998]. The resulting mean lifetime of CH_4 versus tropospheric OH of 10.1 years is very close to the IPCC AR4 recommended value of 9.7 (±20%) years [*Denman et al.*, 2007]. Chemical destruction of CH_4 by OH, Cl, and $O(^1D)$ in the stratosphere is based on the 2D photochemical Max-Planck-Institute (MPI) model [*Brühl and Crutzen*, 1993]. The prescribed concentrations of the radicals are kept annually invariant over the simulation period and are not optimized in the inversion.

[23] The reference inversion over the period 2001–2006 has been split into 6 individual inversions of 14 months each, with overlapping time periods of 2 months between consecutive inversions (this splitting is done because of the very high CPU demand of the inversions). The additional sensitivity inversions (as described in section 3.4) are evaluated for single years only (and run over 14 months starting 1 December of the previous year).

[24] The optimizations are done in 40 m1qn3 iterations, resulting in a reduction of the norm of the gradient (equation (2)) of typically more than 3 orders of magnitude. The inversions are generally performed in 2 cycles: Observational data for which a posteriori mixing ratios assimilated in the first cycle differ by more than 3 sigma are rejected, and subsequently the inversion is repeated with otherwise identical settings. The rationale behind this data rejection is to avoid that single outliers introduce significant biases into the inversion. Typically, ~3% of the data are rejected, which is larger than expected from the 3 sigma criterion, indicating that the overall data uncertainty (equation (4)) is still somewhat underestimated (e.g., due to local sources or local meteorology which are not represented in the model).

[25] While the nonlinear TM5-4DVAR system with the semiexponential PDF of a priori emissions does not provide estimates of the a posteriori uncertainties, we used for this purpose the linear TM5-4DVAR system with Gaussian error distribution [*Meirink et al.*, 2008]. Although this linear system yields somewhat different model solutions (most importantly, it results sometimes in negative a posteriori emissions in regions far from observational constraints), the spatial patterns of the inversion increments are in general very similar to the nonlinear system. Due to the high computational costs of the a posteriori uncertainty estimates (for which we applied 80 conjugate gradient iterations [*Meirink et al.*, 2008]), these have been evaluated only for a single year (2001) for the reference inversion.

3.4. Reference and Sensitivity Inversions

[26] The reference inversion S1 is run over the period 2001–2006 and based on the station set EU-01 (see Table 1). In addition, various sensitivity inversions were done to analyze the robustness of retrieved emissions, as compiled in Table 3. In sensitivity inversions S2 and S3, the spatial correlation length was varied. The inversions S4−S7 investigate the impact of using different sets of monitoring stations, with S4 omitting the semiurban stations London (LON) and Gif sur Yvette (GIF), and S5 omitting Schauinsland (SIL). In S6 and S7, the station sets from inversion scenarios S1 and S3 of *Bergamaschi et al.* [2005] were applied to allow better comparison with the emission estimates of that study. In inversion S8 the sensitivity of results to the a priori inventory is explored, replacing the standard a priori inventory (as described in section 3.3) by the assumption of constant, homogeneous emissions over land (with annual total global emissions of 500 Tg CH_4/yr over land except Antarctica and small constant homogeneous emissions of 17 Tg CH_4/yr over the ocean). In that inversion, the uncertainties of the emissions are set to much larger values (500% per grid cell and month) compared to the standard inversions (100% per grid cell, month and emission group), and the spatial correlation length to a much smaller value of 50 km to give the inversion enough freedom to retrieve regional hot spots.

[27] Finally, in inversion S9 we examine the sensitivity of derived emissions to the applied OH fields, using the OH

Table 3. Reference Inversion and Sensitivity Inversions[a]

Inversion	L_corr (im)	Stations	Period	Description
S1	200	EU-01	2001–2006	reference inversion
S2	100	EU-01	2005	as S1, but spatial correlation length 100km
S3	300	EU-01	2005	as S1, but spatial correlation length 300km
S4	200	EU-02	2001, 2005	as S1, but without LON and GIF
S5	200	EU-03	2005	as S1, but without SIL
S6	200	EU-04	2001	as S1, but stations from inversion S1 of *Bergamaschi et al.* [2005]
S7	200	EU-05	2001	as S1, but stations from inversion S3 of *Bergamaschi et al.* [2005]
S8	50	EU-01	2005	as S1, but homogeneous emissions over land/over ocean resp.
S9	200	EU-01	2005	as S1, but OH fields from *Spivakovsky et al.* [2000]

[a]The different station networks listed in the third column are specified in detail in Table 1.

fields from *Spivakovsky et al.* [2000] instead of those from TM5.

4. Results and Discussion

4.1. Reference Inversion (S1)

[28] Figure 3 shows the average European emissions derived from our reference inversion for the period 2001–2006. Compared to the a priori inventory, pronounced changes in the spatial patterns are apparent. Several emission hot spots in the a priori inventory are significantly reduced in the inversion, especially the emissions in the North Sea (according to the EDGARv4.0 database due to oil and gas production), the large emissions in southern Poland (largely from coal mining in EDGARv4.0), and the emissions around Paris (mainly from gas distribution leaks and waste according to EDGARv4.0). At the same time emissions in rural areas of France are increased along with emissions over the BENELUX countries, western and southern Germany, and Romania.

[29] For further interpretation of the derived emissions, in particular in the context of verification of bottom-up inventories, it is important to analyze the sensitivity of the available observations to the emissions. In Figure 4 (top) we show the sensitivity of the observational network used for the reference inversion, evaluated by the TM5 adjoint model, relating emissions (in kg CH_4 s^{-1}) to the signal detected by the network (in ppb). Generally, the sensitivity is relatively high for Northwest Europe (and, as expected, largest around the individual monitoring stations), but significantly lower for South and East Europe. An alternative way to analyze the observational constraints on the emission estimates is to evaluate the uncertainty reduction determined by the inverse modeling system, i.e., the ratio between a posteriori and a priori uncertainties, as shown in Figure 4 (bottom). Figure 4 (bottom) shows an even more pronounced gradient between the relatively well constrained emissions over northwest Europe, for which uncertainty reductions on the order of 25–50% for emissions from individual model grid cells are calculated compared to south and east Europe, for which over large parts little reduction in uncertainty is achieved. The comparison with Figure 4 (top) illustrates that, although the network shows some (though weak) sensitivity to emissions at larger distances from the monitoring stations, it cannot attribute emissions to individual grid cells at such large distances.

[30] The sensitivity of the observations to emissions has also been analyzed in detail in a concomitant study using synthetic observations which were generated by TM5 forward model simulations and subsequently inverted in the TM5-4DVAR system [*Villani et al.*, 2010]. This study also demonstrated clearly that the available European observations mainly constrain emissions from Northwest Europe (with the 'CS' network of *Villani et al.* [2010] being very similar to the network EU-01 used in this study for the reference inversion).

[31] Based on the described sensitivity analyses, we focus this study on emissions from Northwest European countries: UK and Ireland, BENELUX countries, France and Germany (the total of these countries is hereafter denoted as NWE; for UK and Ireland we generally analyze the sum of both countries, denoted as UK + Ireland).

[32] Annual total emissions derived for these countries are compiled in Table 4 and displayed in Figure 5. For direct comparison with bottom-up inventories of anthropogenic emissions the estimated small contribution of natural sources is subtracted from the derived total emissions (see section 3.3). Figure 5 also includes the previous estimates of *Bergamaschi et al.* [2005] for 2001, which were based on a synthesis inversion. The emissions estimated in that study were ~30% higher for UK + Ireland, ~30% lower for BENELUX, but very close to our reference inversion for France, Germany, and the total of NWE. For better comparability we also performed the 4DVAR inversions with the same set of observations as used by *Bergamaschi et al.* [2005] (sensitivity inversions S6 and S7), resulting in very similar estimates for the country totals as reference inversion S1. The most important difference between the two studies is the inversion technique: While the synthesis inversion can be potentially affected by the aggregation error [*Kaminski et al.*, 2001], this systematic error is minimized in the 4DVAR system allowing the flexible optimization of individual grid cells within the constraints set by the spatial correlation length. Further differences between the two studies include different a priori inventories and different sampling of the observations (*Bergamaschi et al.* [2005] used daily mean values) and uncertainties used for the observations (*Bergamaschi et al.* [2005] estimated the model representativeness error mainly based on the 3D model gradient). Despite these differences, the two studies show good consistency, especially for the NWE total, for which the aggregation error of the synthesis inversion should have a smaller impact than for the estimates of the individual countries.

[33] The extension of the analysis in this study to the time period 2001–2006 shows relatively small variability of derived country totals for the individual years, with a standard deviation below 14% for all countries. This demon-

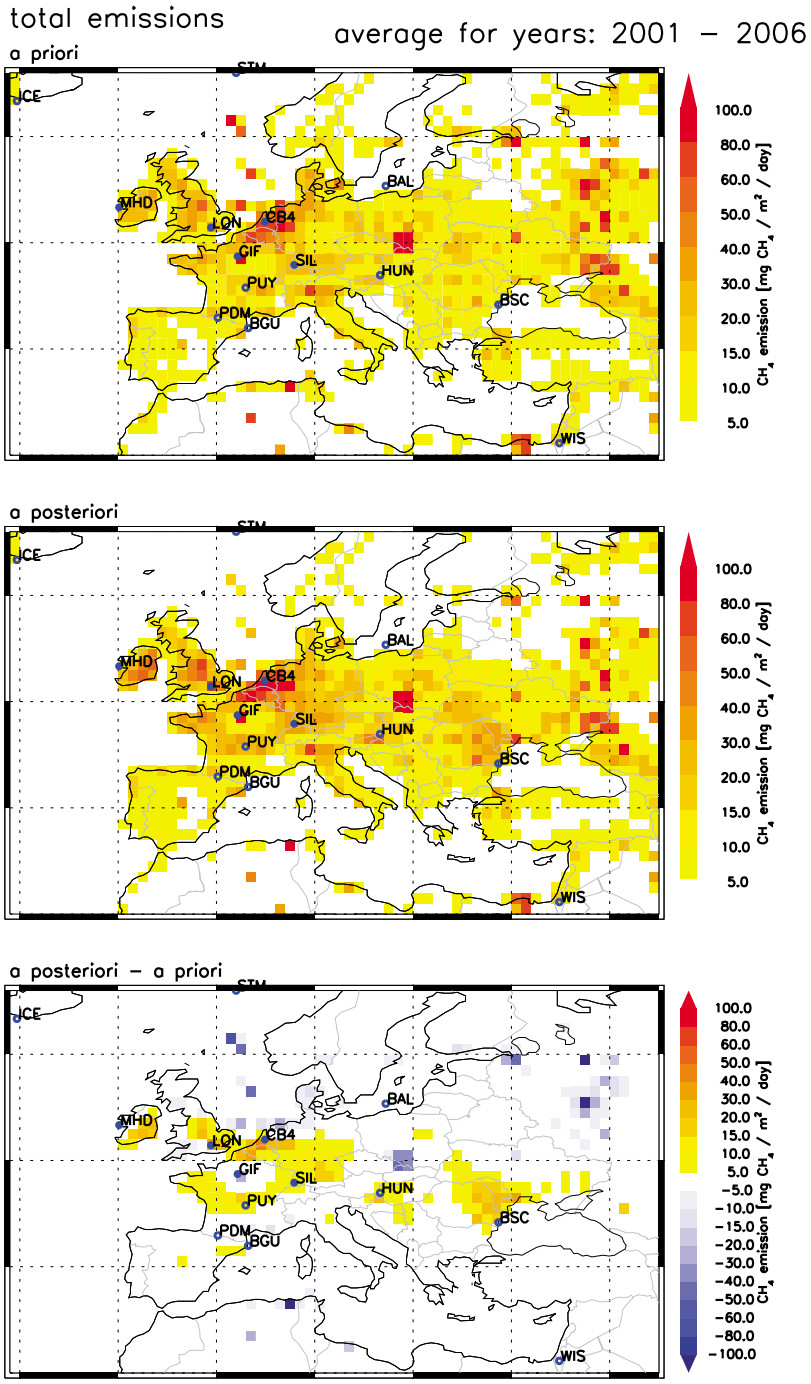

Figure 3. Mean European CH_4 emissions for the period 2001–2006 (total emissions per grid cell): (top) a priori emissions, (middle) a posteriori emissions derived in reference inversion S1, and (bottom) inversion increments (a posteriori − a priori).

strates the robustness of the top-down estimates over this period, assuming that interannual variability of the emissions is low, as can be expected from the dominance of anthropogenic sources in the study area.

[34] The inversion shows a small negative trend of NWE emissions of −0.15 Tg CH_4/yr^2 (2001–2006), compared to −0.24 Tg CH_4/yr^2 in EDGARv4.0 (2001–2005) and −0.39 Tg CH_4/yr^2 for the emissions reported to UNFCCC (2001–2006). However, this period is probably too short for a reliable trend analysis and uncertainties of the derived trends are difficult to estimate. Therefore, the emission trends are not further discussed in this study.

[35] Compared to the EDGARv4.0 inventory, which was used as a priori estimate in the inversion, the a posteriori average emissions for 2001–2006 are 21% higher for NWE (ranging between +18% for UK + Ireland and +28% for Germany). Somewhat larger differences, however, are apparent in comparison with the emissions reported to

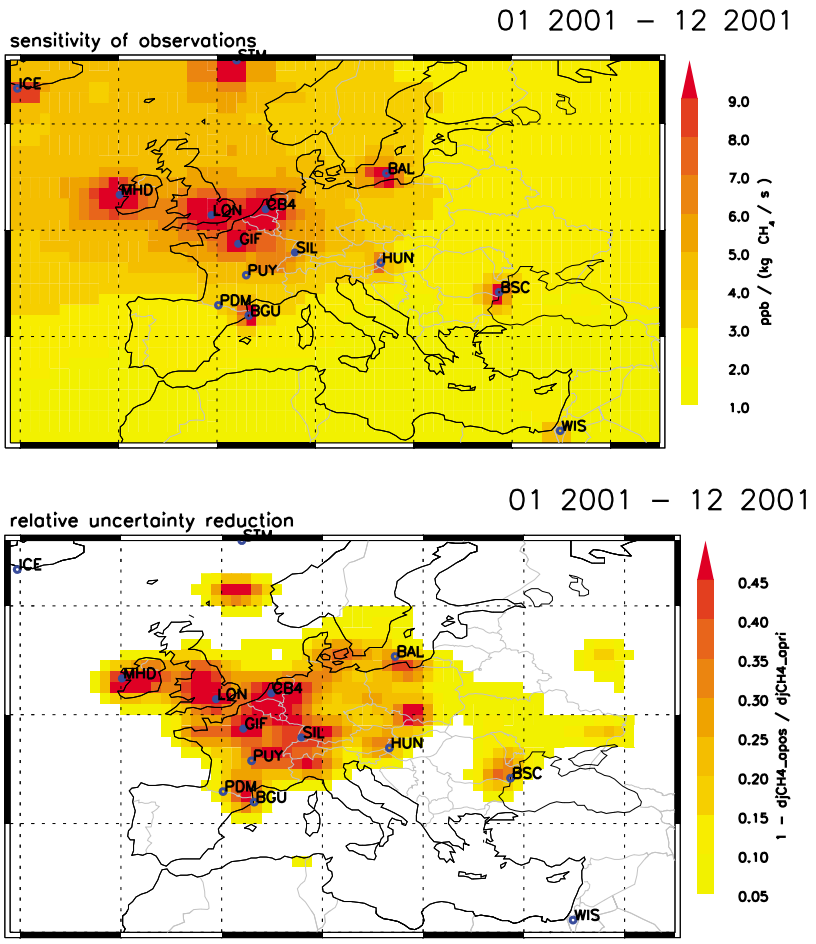

Figure 4. (top) Sensitivity of observational network EU-01 used for the reference inversion S1 evaluated by the TM5 adjoint model; plot shows the average sensitivity for year 2001. (bottom) Calculated reduction of uncertainties of emissions per grid cell ($1 - \Delta jCH_{4\ apos}/\Delta jCH_{4\ apri}$).

UNFCCC. For NWE, the 2001–2006 average derived in the reference inversion is 40% higher than the emissions reported to UNFCCC (which are 14% lower than the EDGARv4.0 values). The best agreement is found for the emissions for UK + Ireland, for which the derived emissions agree within 1%, while the inversion yields 64%, 71%, and 49% higher emissions for BENELUX, France, and Germany, respectively. The countries report also their uncertainty estimates for the major source categories in their national inventory reports (Table 5). Assuming no correlation among the errors of the different categories, the uncertainties for the national total emissions are in the range of ~19–27% (only for Ireland is a smaller uncertainty estimated; uncertainties are given at the 2σ level [*IPCC*, 2000]). We note, however, that there are large differences in uncertainty estimates among countries; for example, the uncertainty estimates range between 12.5% and 62.4% for waste, between 5.9 and 40.3% for enteric fermentation, and between 13.0 and 138.7% for emissions from coal mining (Table 5). The different uncertainty estimates are due to different methodologies applied by different member states (and partly also due to different technologies), but reflect also the uncertainties of the uncertainty estimates. Therefore, we adopt a uniform uncertainty of 30% for the national total emissions in Figure 5.

[36] The uncertainties of the top-down emission estimates are also difficult to estimate. In Table 6 we have compiled the uncertainty estimates for the a posteriori emissions evaluated for reference inversion S1 for year 2001 (based on the additional inversion using the conjugate gradient minimization, as described in section 3.3). These uncertainty estimates represent a mapping of the data uncertainties (defined by equation (4)) to the emissions; that is, they include our estimates of the model representativeness error, but not any further potential systematic model errors, such as errors in model transport. To account for such further errors, we add an additional error term set to 30%. This number is a first estimate, based on preliminary results from a detailed comparison of 4 inverse models currently performed in the European project NitroEurope (http://www.nitroeurope.eu). Clearly, this uncertainty estimate will have to be better quantified based on the ongoing model comparisons and further model validation studies.

[37] Based on the described uncertainty estimates, the top-down emission estimates can be still considered to be consistent with the UNFCCC values (with 2σ ranges of bottom-up and top-down estimates overlapping for all NWE countries), although a clear tendency toward higher top-down values is apparent for all NWE countries except UK + Ireland.

Table 4. Emissions for NWE Countries: UNFCCC Values, a Priori Values From the EDGARv4.0 Database, and a Posteriori for Reference Inversion S1 (2001–2006) (Tg CH_4/yr)

	2001	2002	2003	2004	2005	2006	Average
				UK + Ireland			
UNFCCC	3.67	3.53	3.27	3.16	3.07	3.03	3.29
EDGARv4.0	2.91	2.85	2.86	2.76	2.66	2.66[a]	2.78
S1 (anthrop.)	3.28	3.12	3.32	3.62	3.30	3.10	3.29
S1 (natural)	0.45	0.42	0.46	0.45	0.43	0.45	0.44
				BENELUX			
UNFCCC	1.33	1.26	1.22	1.20	1.17	1.15	1.22
EDGARv4.0	1.81	1.74	1.67	1.68	1.61	1.61[a]	1.69
S1 (anthrop.)	2.00	1.84	1.80	1.91	2.29	2.18	2.00
S1 (natural)	0.04	0.03	0.04	0.04	0.05	0.05	0.04
				France			
UNFCCC	2.86	2.79	2.72	2.64	2.61	2.58	2.70
EDGARv4.0	3.96	3.89	3.86	3.81	3.79	3.79[a]	3.85
S1 (anthrop.)	4.70	4.66	4.61	4.53	4.72	4.45	4.61
S1 (natural)	−0.03	−0.06	−0.03	−0.03	−0.05	−0.03	−0.04
				Germany			
UNFCCC	2.88	2.72	2.52	2.32	2.20	2.10	2.46
EDGARv4.0	3.11	2.99	2.89	2.77	2.72	2.72[a]	2.86
S1 (anthrop.)	3.69	4.08	3.97	3.85	3.79	2.63	3.67
S1 (natural)	−0.02	−0.02	−0.03	−0.02	−0.04	0.01	−0.02
				NWE			
UNFCCC	10.74	10.30	9.74	9.32	9.05	8.86	9.67
EDGARv4.0	11.78	11.47	11.28	11.02	10.78	10.78[a]	11.18
S1 (anthrop.)	13.67	13.70	13.71	13.92	14.10	12.35	13.58
S1 (natural)	0.44	0.38	0.44	0.45	0.38	0.48	0.43

[a]For year 2006, EDGARv4.0 values of 2005 are applied.

[38] Differences are also apparent between the bottom-up inventories, with the EDGARv4.0 estimate for NWE total being 16% higher than the UNFCCC values, but these differences vary among the countries, for example, EDGARv4.0 values for UK + Ireland are 15% lower, but 38% higher for BENELUX and 43% higher for France compared to UNFCCC. Assuming a similar uncertainty for the EDGARv4.0 country totals as for the UNFCCC numbers (~30%), the different bottom-up estimates are still consistent with each other. We note, however, that larger discrepancies exist for individual source categories as compiled in Table 7, especially for waste and oil+gas. For instance, EDGARv4.0 emissions from waste in the UK are only ~10% of the UNFCCC estimate. This is due to the fact that EDGARv4.0 calculates 100% recovery for landfill sites in the UK, which, however, is likely an artifact of the applied methodology: While the total amount of landfill gas recovered is relatively well documented (and broadly consistent between EDGAR and UNFCCC), relatively large uncertainties exist for the estimate of CH_4 production from solid waste and net zero emissions are calculated, if the estimated production does not exceed the recovered landfill gas. To overcome this problem the EDGAR methodology for CH_4 from waste has been updated recently (EDGARv4.1), calculating the recoveries as share percentage reductions, which leads to overall much better agreement with UNFCCC emissions, especially for UK and Ireland (see Table 7).

[39] Furthermore, EDGARv4.0 has generally much higher emissions related to oil + gas compared to UNFCCC, with the largest difference in France (EDGARv4.0 1.43 Tg CH_4/yr; UNFCCC 0.09 ± 0.02 Tg CH_4/yr). While emissions from gas production in France are similar in both inventories, the difference is mainly due to emissions from gas transport and distribution: These are estimated in EDGARv4.0 based on the length of pipelines, the mix of pipeline materials, and material specific emission factors, resulting in a relatively high country total emission of ~1.3 Tg CH_4/yr from gas transport and distribution, while no emissions are reported under this subcategory in the French UNFCCC inventory.

[40] The differences between EDGARv4.0 and UNFCCC for the NWE totals are dominated by the differences in emissions from oil + gas production and distribution (UNFCCC: 0.83 Tg CH_4/yr; EDGARv4.0: 2.83 Tg CH_4/yr).

4.2. Sensitivity Experiments

4.2.1. Dependence of Derived Emissions on Spatial Correlation Length (S2 and S3)

[41] In a first set of sensitivity experiments we explore the impact of the assumed spatial correlation length [*Meirink et al.*, 2008], which was set to 200 km in the reference inversion. Reducing the spatial correlation length to 100 km (sensitivity inversion S2) results in inversion increments on smaller scales, while increasing the spatial correlation length to 300 km (sensitivity inversion S3) leads to the opposite effect. The overall effect on region or country aggregated emissions, however, is very small (auxiliary material Figure S1), and the derived country totals differ only very little from the reference inversion S1 (Figure 5 and Table 8), generally by less than 3.3% for the NWE countries discussed here.

4.2.2. Dependence of Derived Emissions on Set of Stations (S4−S7)

[42] The next set of sensitivity experiments investigates the impact of the atmospheric network used on the derived emissions. In particular monitoring stations very close to CH_4 sources could introduce some systematic error, since local sources and local subgrid-scale meteorology are not resolved by the model. Although the potential systematic error arising from the subgrid-scale variability of emissions is estimated by our model representativeness error (see section 3.2), it cannot be ruled out that in case of significant sources near the monitoring station some bias is introduced in the inversion. In sensitivity inversion S4 we therefore omit the semiurban sites LON (close to London) and GIF (close to Paris) which could be affected by such local sources (e.g., leaks in urban natural gas distribution networks, or landfill sites close to the city). The emissions derived in S4 show some differences in the spatial patterns compared to the reference inversion S1, with lower emissions around London, but higher emissions around Paris (Figure 6). However, these changes close to the omitted stations are partly compensated by inversion increments at larger distances, leading to relatively small changes only in the country totals (maximum difference of 10% for UK + Ireland, and 5% for France compared to S1, evaluated for years 2001 and 2005). The fact that higher emissions are retrieved around Paris without GIF (in 2005) suggests that it is very unlikely that this station is influenced significantly by local sources (which should lead to the opposite effect). Omitting this station results in emission estimates closer to the a priori emission inventory in the footprint area of this station. For 2001, the differences between S4 and S1 are

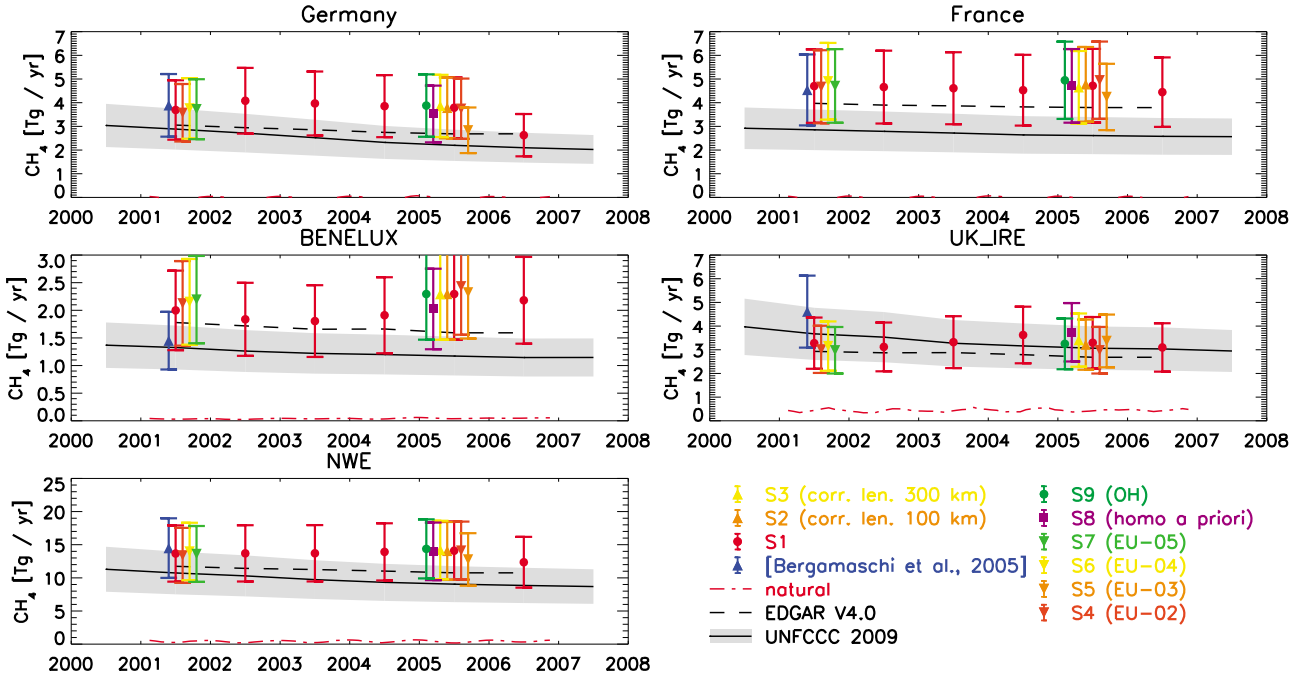

Figure 5. Annual total CH_4 emissions for the NWE countries. The colored symbols represent the emission estimates derived from the reference inversion over 2001–2006 and the various sensitivity inversions performed for 2001 and 2005. The values represent annual anthropogenic emissions (except for S8, for which the total emissions are shown). Estimates of natural sources (including soil sink) are shown by the red dash-dotted line (a posteriori, which, however, largely depends on the a priori information on the natural sources and sinks). The blue symbol shows the previous estimates of *Bergamaschi et al.* [2005]. Black solid line represents UNFCCC values (as reported in 2009), and the gray-shaded area is their assumed uncertainty of ~30%. The black dashed line shows national total anthropogenic emissions from the EDGARv4.0 inventory.

smaller than 2005 (auxiliary material Figure S2), especially over France, which might be partly due to a data gap at GIF in the first months of 2001.

[43] Further systematic errors could be introduced by mountain stations, since the local topography is in general not resolved by the model. In sensitivity inversion S5, we omitted Schauinsland (SIL), located in the Black Forest at 1205 m asl. The resulting derived emissions show some differences in the spatial patterns over France compared to the reference inversion and somewhat smaller total emissions from France (10% lower than S1). However, larger differences are derived for Germany, with a 25% lower country total compared to S1. This is most likely due to the weaker sensitivity to the German emissions of the observational network EU-03 without SIL, resulting in a model solution closer to the German a priori emissions. In the absence of further German stations in EU-03, it is therefore difficult to disentangle the impact of potential systematic errors in the simulation of the mountain station SIL on the derived German emissions (in the reference inversion S1 based on the EU-01 network) from the different network sensitivity. In further sensitivity experiments we therefore explored also the effect of changing the sampling altitude of SIL in the model. While the standard algorithm (based on the geopotential heights of the vertical layers for the 1° × 1° resolution) puts SIL at 559 m above the TM5 model surface, we shifted this default height by −200 and +200 m in two additional sensitivity experiments shown in the auxiliary material (Figure S3). As expected, decreasing the altitude results in lower emissions retrieved for France and Germany, while increasing the altitude leads to the opposite effect. The impact on the derived total emission for France and Germany is however not very large (maximum difference for France 13% and for Germany 14% compared to S1), i.e., for Germany smaller than the difference of 25% between sensitivity inversion S5 and the reference inversion. This suggests that for inversion S5 indeed the weaker sensitivity of the observational network to the German emissions is the dominant effect resulting in derived emissions for Germany closer to the a priori inventory.

[44] Finally, we applied the station sets used by *Bergamaschi et al.* [2005] to allow direct comparison with the emission estimates derived in that study. These station sets (EU-04 and EU-05) include further German sites operated by the Germany Umweltbundesamt (which were unfortunately discontinued (ZGT, DEU) or changed their monitoring position (monitoring station Zugspitze (2960 m asl) moved to Schneefernerhaus (2656 m asl) at the end of 2001) and could therefore not be used for our extended analysis period 2001–2006. On the other hand, our reference station set EU-01 includes a number of new stations (LON, PUY, PDM, BGU) which were not available in the study of *Bergamaschi et al.* [2005]. The sensitivity inversions S6 and S7 performed with the station sets EU-04 and EU-05 show, similar to S4, some changes in the derived spatial emission patterns (auxiliary material Figure S2), but overall only

Table 5. Uncertainty Estimates (2σ) for Emissions Reported to UNFCCC

	Unit	UK	IRE	NL	BEL	France	Germany	NWE[a]
Solid Fuel								
Emission (2001–2006)	Tg CH_4/yr	0.25	0.00	0.00	0.00	0.03	0.37	0.65
Relative uncertainty	%	13.0			60.2		138.7	83.3
Absolute uncertainty	Tg CH_4/yr	0.03	0.00	0.00	0.00	0.00	0.51	0.54
Oil + Gas								
Emission (2001–2006)	Tg CH_4/yr	0.31	0.01	0.04	0.02	0.09	0.35	0.81
Relative uncertainty	%	15.0	10.3	25.0–53.0	31.6–50.2	18.0	64.7–75.5	37.7
Absolute uncertainty	Tg CH_4/yr	0.05	0.00	0.01	0.01	0.02	0.22	0.31
Enteric Fermentation								
Emission (2001–2006)	Tg CH_4/yr	0.77	0.44	0.30	0.18	1.38	0.84	3.90
Relative uncertainty	%	20.0	11.4	15.2	40.3	40.3	5.9	23.7
Absolute uncertainty	Tg CH_4/yr	0.15	0.05	0.05	0.07	0.56	0.05	0.93
Manure Management								
Emission (2001–2006)	Tg CH_4/yr	0.14	0.11	0.13	0.08	0.67	0.26	1.39
Relative uncertainty	%	30.0	11.2	69.7	41.2	50.2	11.6	39.0
Absolute uncertainty	Tg CH_4/yr	0.04	0.01	0.09	0.03	0.34	0.03	0.54
Solid Waste								
Emission (2001–2006)	Tg CH_4/yr	1.08	0.07	0.32	0.05	0.31	0.59	2.42
Relative uncertainty	%	48.4	62.4	34.0	50.0	53.9	12.5	38.9
Absolute uncertainty	Tg CH_4/yr	0.52	0.05	0.11	0.02	0.17	0.07	0.94
Wastewater								
Emission (2001–2006)	Tg CH_4/yr	0.04	0.00	0.01	0.01	0.06	0.01	0.12
Relative uncertainty	%	50.0	31.6	32.0	72.8	104.4	45.3	75.0
Absolute uncertainty	Tg CH_4/yr	0.02	0.00	0.00	0.00	0.06	0.00	0.09
Total								
Total major categories[b]	Tg CH_4/yr	2.58	0.63	0.79	0.33	2.55	2.41	9.29
Total all anthropogenic[c]	Tg CH_4/yr	2.65	0.64	0.85	0.35	2.70	2.46	9.65
Total uncertainty[d]	Tg CH_4/yr	0.55	0.07	0.15	0.08	0.67	0.56	1.56
Relative uncertainty[d]	%	21.3	11.0	18.5	24.9	26.5	23.4	16.8
Relative uncertainty[e]	%	23		16–25[f]				

[a]For aggregation of uncertainties for emissions from individual countries to the NWE uncertainties, correlated errors are assumed (for emissions of same categories). In reality, the errors may be only partially correlated.
[b]Major categories are the individual categories listed in this table.
[c]Country total of all anthropogenic emissions as reported to UNFCCC (2001–2006 mean).
[d]Uncertainty of total emissions estimated from the uncertainties given for the listed major individual source categories, assuming no correlation among the errors of different categories.
[e]Estimated uncertainty of total emissions from national inventory reports (available only for a few countries).
[f]For the Netherlands, two different values are given for the overall uncertainty of national total CH_4 emissions. The higher values include also some correlations among different categories and an estimate of potential errors due to nonreported sources [*van der Maas et al.*, 2009].

small differences in the country totals (differences generally less than 10% compared to S1; Table 8).

4.2.3. Dependence of Derived Emissions on a Priori Emission Inventory (S8)

[45] Beside the observational constraints, the applied a priori emission inventories play an important role, since they are predefining the potential solution space for the a posteriori emissions. The emission uncertainties are generally specified as a percentage of the a priori emissions (see section 3.3). Thus, on the one hand, grid cells with very low a priori emissions usually cannot turn into grid cells with very high a posteriori emissions. That is, significant point sources which are not included in the a priori inventory may not be properly derived in the inversion. On the other hand, small fractional inversion increments at emission hot spots may have a large regional impact with only small costs in the parameter part of the cost function. Hence, unless such hot spots are constrained by nearby observations, the inversion may erroneously attribute the inversion increments largely to such hot spots. In sensitivity inversion S8 we replace our detailed standard a priori emission inventory by a simple a priori emission inventory with homogeneous emissions mostly over land (as described in section 3.4) with very large uncertainties to enable the inversion to be driven largely by the observational constraints. For the NWE countries, inversion S8 yields regional emission patterns which are very consistent with our reference inversion (Figure 7). Despite differences at the grid scale, which are

Table 6. Uncertainty Estimates (2σ, %) for Emissions Derived by the TM5–4DVAR Inverse Modeling System

	Calculated Uncertainty	Potential Additional Uncertainty	Overall Uncertainty
UK + Ireland	14.1	~30	~33
BENELUX	20.5	~30	~36
France	13.7	~30	~33
Germany	15.2	~30	~34
NWE	6.6	~30	~31

Table 7. Contribution of Different Source Categories (2001–2005 Average) in UNFCCC and EDGAR Emission Inventories[a]

	Coal	Oil + Gas	Enteric Fermentation + Manure	Waste	Other	Total
UK						
UNFCCC	0.26	0.32	0.92	1.14	0.07	2.70
EDGARv4.0	0.14	0.67	1.21	0.11	0.04	2.16
EDGARv4.1				1.32		3.37
Ireland						
UNFCCC	0.00	0.01	0.55	0.07	0.01	0.64
EDGARv4.0	0.00	0.07	0.56	0.01	0.00	0.64
EDGARv4.1				0.08		0.71
BENELUX						
UNFCCC	0.00	0.06	0.70	0.39	0.08	1.24
EDGARv4.0	0.00	0.27	0.78	0.62	0.04	1.70
EDGARv4.1				0.52		1.60
France						
UNFCCC	0.04	0.09	2.05	0.38	0.16	2.72
EDGARv4.0	0.02	1.43	1.77	0.48	0.15	3.86
EDGARv4.1				0.32		3.70
Germany						
UNFCCC	0.39	0.35	1.11	0.63	0.05	2.53
EDGARv4.0	0.29	0.39	1.45	0.67	0.10	2.89
EDGARv4.1				0.88		3.10
NWE						
UNFCCC	0.69	0.83	5.33	2.62	0.37	9.83
EDGARv4.0	0.45	2.83	5.76	1.89	0.33	11.26
EDGARv4.1				3.12		12.49

[a]In addition to EDGARv4.0 (which has been used as a priori emission inventory in this study), the recent update of EDGAR waste emissions are also compiled (EDGARv4.1). Units are Tg CH_4/yr.

not unexpected in the absence of a clear 'guiding' by the detailed a priori inventories, major regional-scale patterns are consistent with S1, in particular the enhanced emissions over the BENELUX area and Southern UK. Furthermore, the country totals derived in S8 are generally fairly consistent with the reference inversion (Table 8 and Figure 5). Note that the country totals compiled for S8 refer to the total emissions (since in the absence of any detailed a priori information no differentiation can be made between natural and anthropogenic sources). Our a priori inventories, however, suggest that for the NWE countries the natural emissions are generally very small (<3% for NWE countries except UK + Ireland, for which the natural sources are estimated to contribute ~15%). Correcting for these natural emissions, the anthropogenic emissions estimated in S8 for UK + Ireland are virtually identical to the reference inversion.

[46] The good agreement between the 'free inversion' S8 and the reference inversion S1 demonstrates that the large-scale top-down estimates for the NWE countries are strongly constrained by the observational data, while the applied detailed a priori inventories have a relatively small impact on the derived country totals. This finding is of particular importance in the context of verification, since such 'free inversions' can be considered as truly independent top-down emission estimates, apart from the general assumption that emissions are mostly over land.

[47] The 'free inversion', however gives reasonable results only in regions which are sufficiently constrained by the observational network. For example, some positive biases are visible over Scandinavia and northern Africa, where the homogeneous a priori emissions are apparently too high. Moreover, emission hot spots far away from the monitoring stations cannot be properly retrieved.

4.2.4. Dependence of Derived Emissions on OH Sink (S9)

[48] Finally we investigated the impact of CH_4 sinks (sensitivity inversion S9) by replacing the standard TM5 OH fields with those from *Spivakovsky et al.* [2000], with a somewhat different spatiotemporal distribution and 4% higher globally averaged OH concentrations (weighted with the reaction rate with CH_4). The impact on the derived spatial emission patterns (auxiliary material Figure S4) and the country totals (Table 8 and Figure 5) is generally relatively small, with a maximum difference for the NWE country totals of 5% (and 2% for total NWE). One might have expected an even smaller sensitivity given the strong observational constraints close to the emissions and the negligible impact of the OH sink at the short time scales

Table 8. Sensitivity Inversions[a]

	Year 2001				Year 2005						
	S1	S4	S6	S7	S1	S2	S3	S4	S5	S8	S9
UK + Ireland	3.28	3.02	3.15	2.98	3.30	3.22	3.41	2.98	3.37	3.74	3.25
BENELUX	2.00	2.13	2.15	2.19	2.29	2.30	2.29	2.43	2.32	2.02	2.29
France	4.70	4.67	4.91	4.71	4.72	4.78	4.65	4.95	4.24	4.71	4.95
Germany	3.69	3.58	3.76	3.73	3.79	3.78	3.86	3.75	2.83	3.52	3.88
NWE	13.67	13.39	13.98	13.61	14.10	14.07	14.21	14.11	12.78	14.00	14.37

[a]Annual anthropogenic emissions in Tg CH_4/yr; for S8 the compiled values refer to annual total emissions.

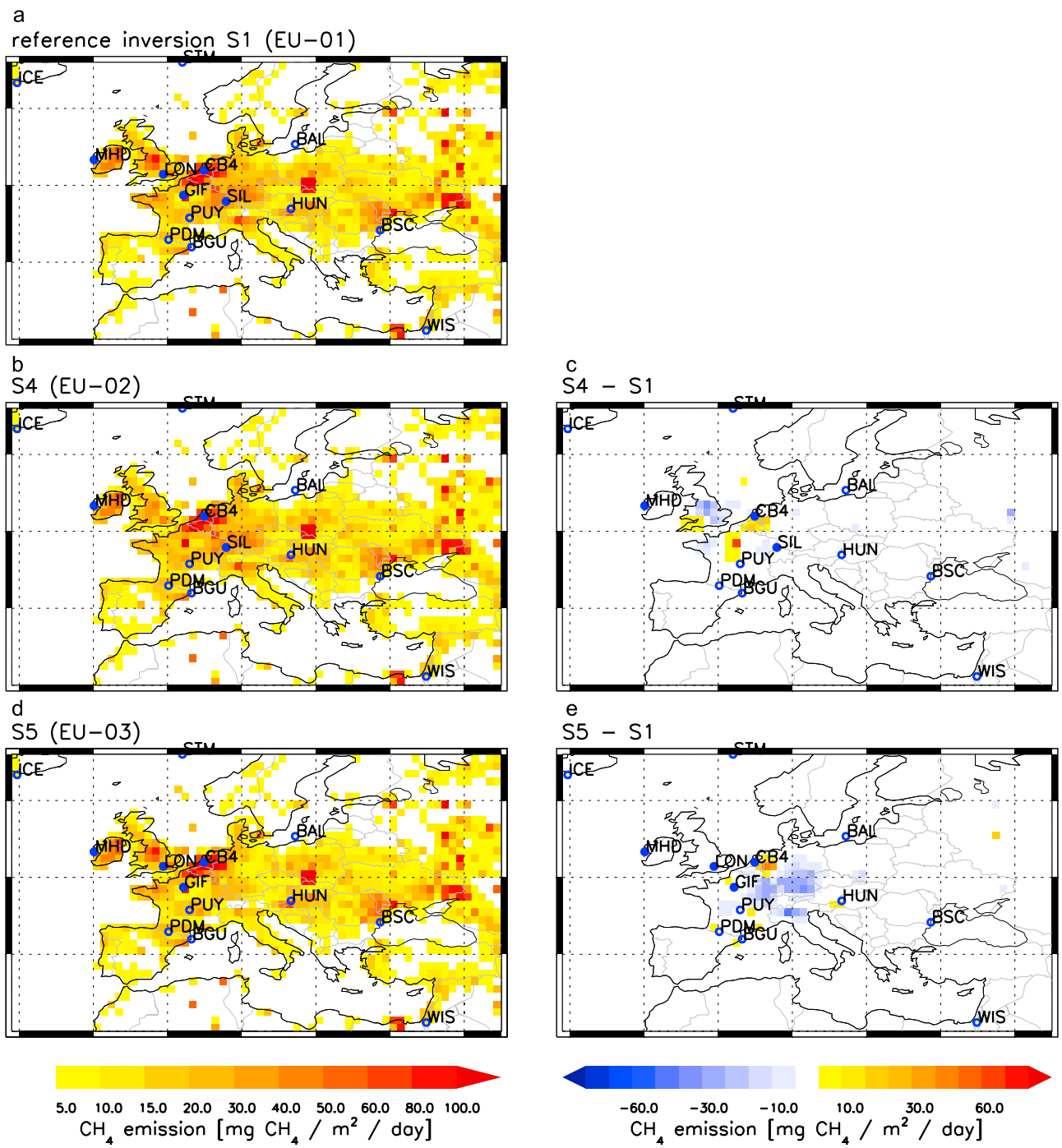

Figure 6. Sensitivity experiments investigating the impact of the observational network. (a) Mean emissions derived in reference inversion S1 for year 2005. (b) Mean emissions derived in sensitivity inversion S4 based on network EU-02. (c) Difference between S4 and S1. (d) Mean emissions derived in sensitivity inversion S5 based on network EU-03. (e) Difference between S5 and S1.

(~hours to days) between emissions from the NWE domain and the detection of this signal at the European monitoring stations. Apparently, the different 3D distributions of the two applied OH fields have some impact on the derived global emissions, which then may indirectly slightly influence the emissions derived in the European domain.

4.3. Validation of Simulated Vertical CH_4 Gradients

[49] Realistic simulation of atmospheric transport processes, and in particular vertical mixing, is very critical for inverse modeling based emission estimates [*Stephens et al.*, 2007]. In a previous study, global TM5 model fields optimized by NOAA surface observations and SCIAMACHY satellite data were validated comprehensively, using inde-

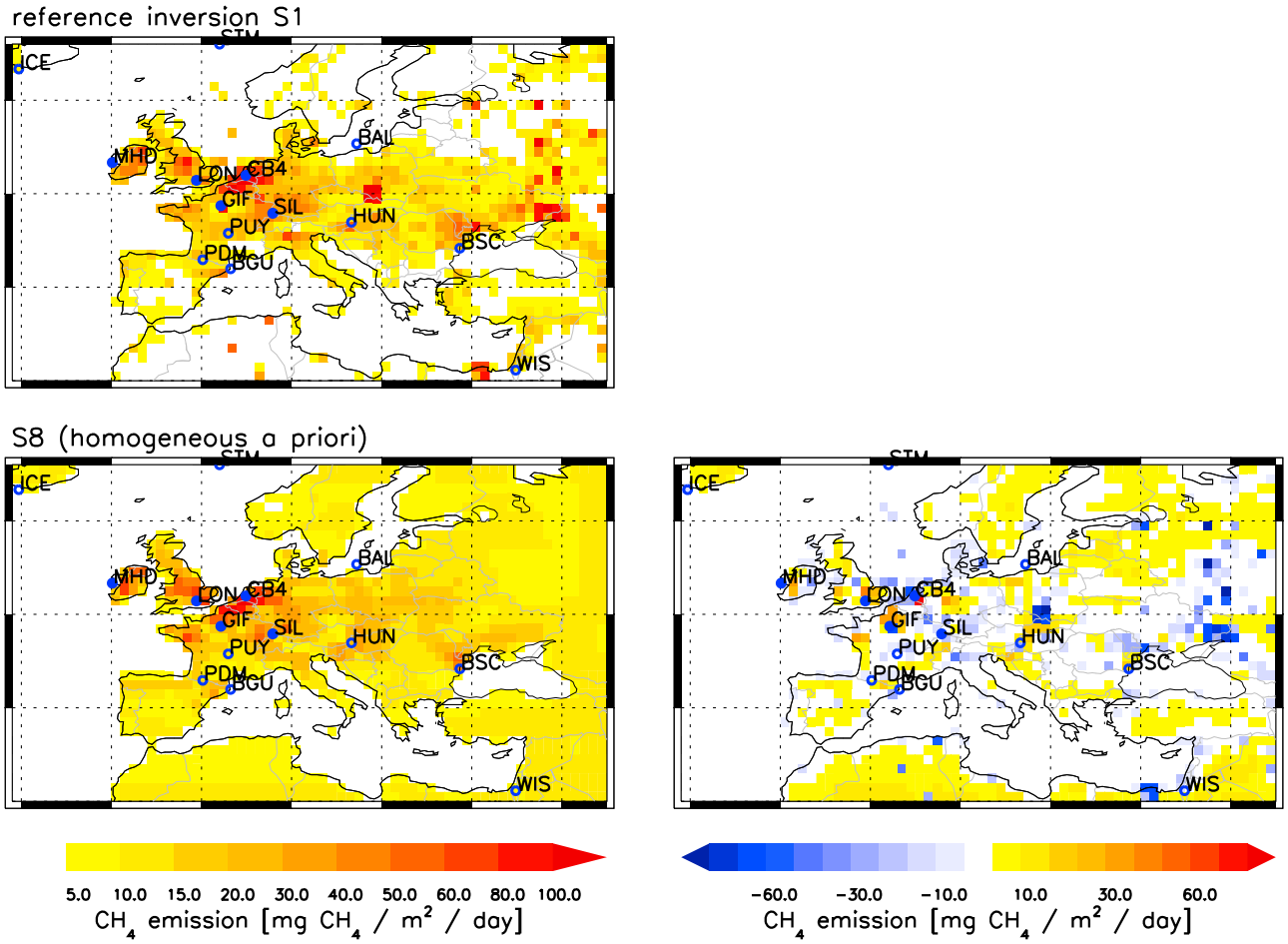

Figure 7. Sensitivity experiments investigating the impact of the a priori emission inventory. (top left) Mean emissions derived in reference inversion S1 for year 2005. (bottom left) Mean emissions derived in sensitivity inversion S8, based on homogeneous a priori emissions over land. (bottom right) Difference between S8 and S1.

pendent observations from ship cruises, aircraft and balloon profiles, showing overall good agreement [*Bergamaschi et al.*, 2009]. In the present study we use additional European aircraft profiles for further validation of model fields, particularly over the European domain (Table 2). The profile sites Orleans (ORL) and Hungary (HNG) are very close to surface monitoring stations assimilated in the inversion (GIF and HNG, respectively), while the Scottish site Griffin (GRI) is relatively far away from the applied stations. All 3 sites show good agreement between measurements and model simulations for the annual average gradient (Figure 8), demonstrating that the vertical gradient is simulated realistically in the model. The sites ORL and HNG show large average gradients of 50–100 ppb between the surface and the free troposphere, pointing to significant regional CH_4 sources, while GRI shows a much smaller average gradient (~10–20 ppb).

5. Conclusions

[50] European CH_4 emissions from northwest European (NWE) countries have been estimated for the period 2001–2006, using 11 European monitoring stations (including 5 stations with continuous measurements) and further 39 global sites for constraining global background mixing ratios. Our multiannual analysis shows relatively small variability of derived country totals for the individual years, demonstrating the robustness of the top-down estimates over this period. The new emission estimates based on the TM5–4DVAR inverse modeling system show good consistency with the previous synthesis inversion [*Bergamaschi et al.*, 2005], especially for the NWE total (agreement within 6%). The major advantage of the 4DVAR system is the flexible optimization of emissions from individual model grid cells, minimizing the aggregation error, and hence allowing more reliable estimates for individual countries. Use of different sets of stations results in some differences in the derived spatial emission patterns, largely reflecting varying sensitivities of the different networks to the observations. In general, however, the estimates for the NWE country totals are relatively robust and further analysis of the network sensitivity demonstrates that the observations used in the reference inversion provide strong constraints on the emissions from the NWE countries. This is also shown in our 'free inversion' (sensitivity inversion S8 with homogeneous a priori emissions over land), yielding country totals

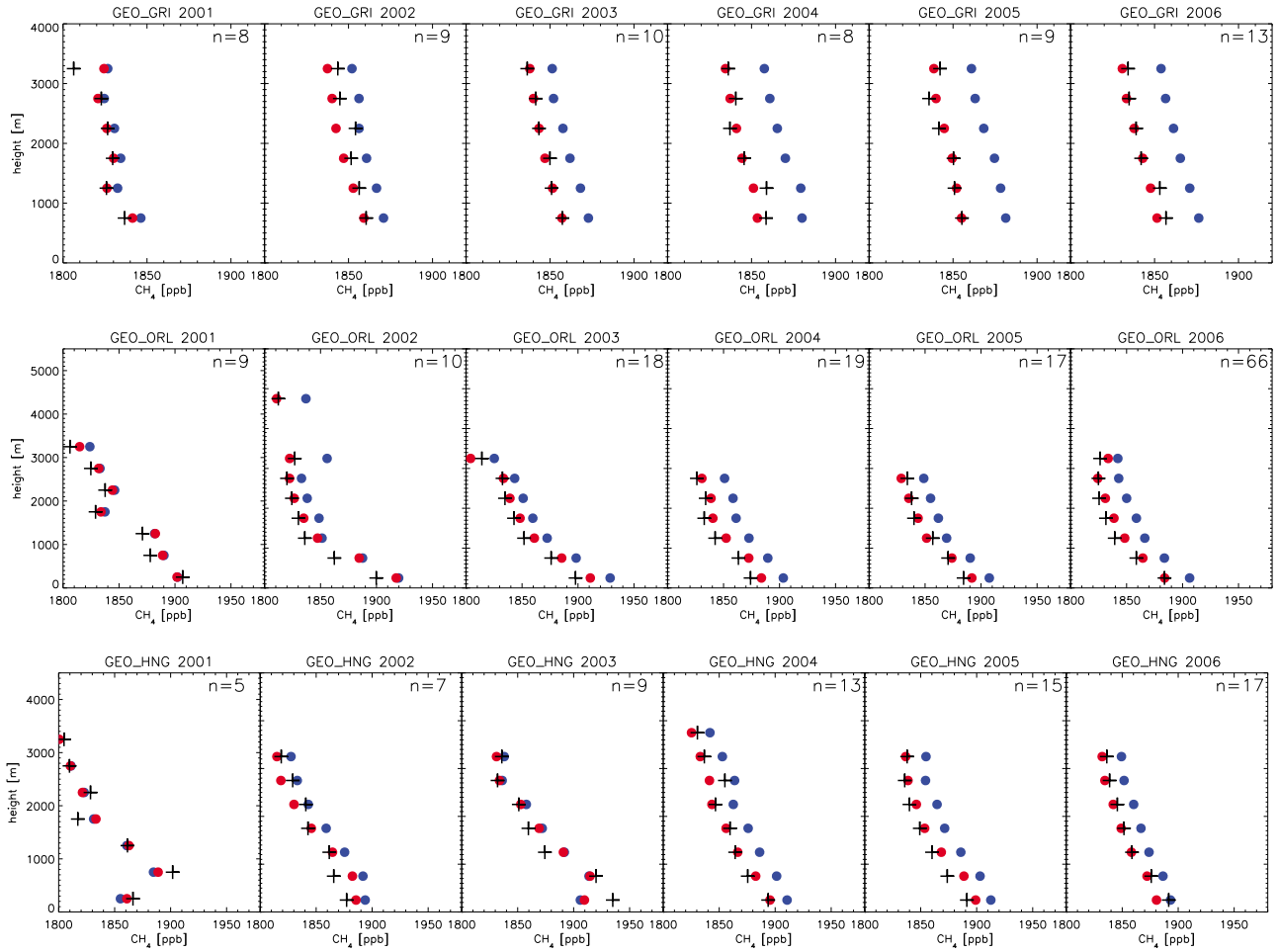

Figure 8. CarboEurope aircraft profiles used for validation of simulated CH_4 mixing ratios over Europe. Black symbols: measurements; blue solid circles: a priori simulations; red solid circles: a posteriori simulations. Annual average values are shown, vertically averaged in 500 m bins, with the number of daily profiles per year given by n (in a few cases, however, the number of samples per altitude bin is smaller than n).

very similar to the reference inversion. Furthermore, this 'free inversion' yields major regional emission patterns (in particular the pronounced emissions over BENELUX) consistent with the reference inversion, but also consistent with the bottom-up inventories. This is in particular important in the context of verification, aiming at top-down emission estimates independent from bottom-up emission inventories usually used as a priori estimates.

[51] Our emission estimates for the NWE countries agree in general better with the EDGARv4.0 emissions estimates (difference of 21% for NWE total; reference inversion S1) than with the UNFCCC values (difference of 40% for NWE total). The recent update of CH_4 waste emissions in the EDGAR inventory (EDGARv4.1) further improves the agreement with the inverse modeling estimate for the NWE total (difference 11%). Higher emissions compared to UNFCCC are retrieved especially for BENELUX, France and Germany (64%, 71%, and 49% respectively), while an almost perfect agreement was found for UK + Ireland. Also the EDGARv4.0 estimates are higher for BENELUX (+38%), France (+43%) and Germany (+17%) than UNFCCC values. Conclusions regarding the consistency between the top-down and bottom-up estimates, however, clearly depend on the assumed uncertainties, which are currently not very well defined. Assuming uncertainties on the order of 30% for both bottom-up and top-down emission approaches, the different estimates can be still reconciled with each other. We note however, that the uncertainties reported in the national inventory reports are somewhat smaller (~19 to 27% for NWE countries, except Ireland for which only ~11% are estimated) and might be underestimated. Furthermore, the uncertainty estimates for individual categories show considerable differences among countries. At the same time, model uncertainties are notoriously difficult to estimate. In this study we adopted model uncertainties of ~31–36% for the NWE countries, based on the calculated uncertainties (which reflect the observational constraints, taking into account the estimated model representativeness error) and potential additional model errors, for example, due to errors in model transport (based on preliminary results from an ongoing model comparison). Verification (or falsification) of bottom-up inventories in a strict sense, however, will clearly require better quantification of uncertainties for both bottom-up and top-down approaches.

[52] Considerable differences between EDGARv4.0 and UNFCCC were found for some source categories, which in some cases appear to be outside the uncertainties given for the individual categories. While the recent update of CH_4 waste emissions in the EDGAR inventory (EDGARv4.1) results in an overall better agreement with UNFCCC emissions reported for the waste sector, large differences are apparent especially for oil+gas production and distribution. Thus, there is an obvious need to clarify these differences in the bottom-up estimates, but also to better quantify emissions from individual source categories by independent top-down approaches, for example, by dedicated local and regional experiments investigating these source types in more detail (e.g., urban gas distribution networks, landfill sites or coal mines [*Hensen and Scharff*, 2001; *Kirchgessner et al.*, 1993; *Lelieveld et al.*, 2005; *Shorter et al.*, 1996]).

[53] Emissions derived from the previous synthesis inversion [*Bergamaschi et al.*, 2005] showed large differences compared to UNFCCC values, particularly for the UK (with emissions estimated for UK + Ireland 65% higher than UNFCCC numbers reported in the 2004 submission). The very good agreement found in the present study is the combined effect of a lower top-down estimate (−28.9% compared to *Bergamaschi et al.* [2005]), and the considerable revision of the UK inventory [*Baggott et al.*, 2006] with 38.6% higher emissions reported in the 2009 inventory report compared to the 2004 report. Also the German CH_4 inventory was substantially revised in the past, with an increase by ~60% in the 2004 submission [*Federal Environment Agency*, 2004], followed 2006 again by a significant downward correction [*Federal Environment Agency*, 2006] (decrease of ~27% compared to the 2004 submission).

[54] The substantial uncertainties of bottom-up inventories are mainly the result of the uncertainties in emission factors of major source categories. Therefore, independent verification by top-down approaches is indispensable and is likely to play an important role for post-Kyoto international agreements on emissions reductions. Verification is essential to monitor the compliance of all parties, in order to ensure the benefit for the global climate. Furthermore, under the existing and further evolving emission trading systems also significant monetary value is involved.

[55] A central prerequisite for independent verification is the availability of long-term, high-quality atmospheric measurements, and, on the European scale, the further extension of the network, especially in South and East Europe, which is currently poorly monitored. At the same time inverse models need to be further improved (e.g., spatial resolution) and their overall uncertainties better quantified, for example, using ensemble inversions based on independent inverse models.

[56] **Acknowledgments.** We thank ECMWF for providing computing resources under the special project "Inverse Modelling of Atmospheric CH_4 and N_2O." We are grateful to Ludwig Ries and Karin Uhse for provision of observational data from the German UBA monitoring network. We thank Ingeborg Levin for comparison of the continuous measurements at Schauinsland with independent flask samples and for helpful comments on the manuscript. We are grateful to the Laboratoire de Météorologie Physique/Observatoire de Physique du Globe de Clermont-Ferrand (LaMP/OPGC) for taking air samples at PUY, Laboratoire d'Aérologie/Observatoire Midi Pyrénées (LA/OMP) for sampling at PDM, School of GeoSciences/University of Edinburgh for sampling at GRI, the Hungarian Meteorological Service for sampling at HNG, and the Institut Català de Ciències del Clima (IC3) for sampling at BGU. We thank Adrian Leip and Bernd Gugele for discussion of uncertainties of UNFCCC emissions. Furthermore, we thank Valerio Pagliari and Fulgencio Sanmartin for assistance with the EDGARv4.0 database and Greet Janssens-Maenhout and Jos Olivier for the EDGARv4.1 update of waste emissions.

References

Baggott, S. L., et al. (2006), UK Greenhouse Gas Inventory, 1990 to 2004, AEA Technol., Harwell, U. K.

Bergamaschi, P. (Ed.) (2007), Atmospheric monitoring and inverse modelling for verification of national and EU bottom-up GHG inventories—Report of the workshop "Atmospheric Monitoring and Inverse Modelling for Verification of National and EU Bottom-up GHG Inventories" under the mandate of Climate Change Committee Working Group I, report, 153 pp., Eur. Comm. Joint Res. Cent., Ispra, Italy. (Available at http://ccu.jrc.ec.europa.eu/IMWS2/report/IMWS2_report_final.pdf)

Bergamaschi, P., M. Krol, F. Dentener, A. Vermeulen, F. Meinhardt, R. Graul, M. Ramonet, W. Peters, and E. J. Dlugokencky (2005), Inverse modelling of national and European CH_4 emissions using the atmospheric zoom model TM5, *Atmos. Chem. Phys.*, *5*, 2431–2460, doi:10.5194/acp-5-2431-2005.

Bergamaschi, P., et al. (2009), Inverse modeling of global and regional CH_4 emissions using SCIAMACHY satellite retrievals, *J. Geophys. Res.*, *114*, D22301, doi:10.1029/2009JD012287.

Brühl, C., and P. J. Crutzen (1993), The MPIC 2D model, *NASA Ref. Publ.*, *1292*, 103–104.

Committee on Methods for Estimating Greenhouse Gas Emissions (2010), *Verifying Greenhouse Gas Emissions: Methods to Support International Climate Agreements*, 125 pp., Natl. Acad., Washington, D. C. (Available at http://www.nap.edu/catalog/12883.html)

Cunnold, D. M., et al. (2002), In situ measurements of atmospheric methane at GAGE/AGAGE sites during 1985–2000 and resulting inferences, *J. Geophys. Res.*, *107*(D14), 4225, doi:10.1029/2001JD001226.

Denman, K. L., et al. (2007), Couplings between changes in the climate system and biogeochemistry, in *Climate Change 2007: The Physical Science Basis. Contribution of Working Group I to the Fourth Assessment Report of the Intergovernmental Panel on Climate Change*, edited by S. Solomon et al., pp. 501-587, Cambridge Univ. Press, Cambridge, U. K.

Dlugokencky, E. J., S. Houweling, L. Bruhwiler, K. A. Masarie, P. M. Lang, J. B. Miller, and P. P. Tans (2003), Atmospheric methane levels off: Temporary pause or a new steady-state?, *Geophys. Res. Lett.*, *30*(19), 1992, doi:10.1029/2003GL018126.

Dlugokencky, E. J., R. C. Myers, P. M. Lang, K. A. Masarie, A. M. Crotwell, K. W. Thoning, B. D. Hall, J. W. Elkins, and L. P. Steele (2005), Conversion of NOAA atmospheric dry air CH_4 mole fractions to a gravimetrically prepared standard scale, *J. Geophys. Res.*, *110*, D18306, doi:10.1029/2005JD006035.

Dlugokencky, E. J., et al. (2009), Observational constraints on recent increases in the atmospheric CH_4 burden, *Geophys. Res. Lett.*, *36*, L18803, doi:10.1029/2009GL039780.

Federal Environment Agency (2004), German Greenhouse Gas Inventory 1990–2002, National inventory report 2004, Berlin.

Federal Environment Agency (2006), National inventory report for the German Greenhouse Gas Inventory 1990–2004, Dessau, Germany.

Forster, P., et al. (2007), Changes in atmospheric constituents and in radiative forcing, in *Climate Change 2007: The Physical Science Basis. Contribution of Working Group I to the Fourth Assessment Report of the Intergovernmental Panel on Climate Change*, edited by S. Solomon et al., pp. 131-234, Cambridge Univ. Press, Cambridge, U. K.

Gilbert, J. C., and C. Lemaréchal (1989), Some numerical experiments with variable-storage quasi-Newton algorithms, *Math. Program.*, *45*, 407–435, doi:10.1007/BF01589113.

Hensen, A., and H. Scharff (2001), Methane emission estimates from landfills obtained with dynamic plume measurements, *Water Air Soil Pollut. Focus*, *1*(5/6), 455–464, doi:10.1023/A:1013162129012.

Houweling, S., F. Dentener, and J. Lelieveld (1998), The impact of nonmethane hydrocarbon compounds on tropospheric photochemistry, *J. Geophys. Res.*, *103*(D9), 10,673–10,696, doi:10.1029/97JD03582.

Intergovernmental Panel on Climate Change (IPCC) (1996), Revised 1996 IPCC guidelines for national greenhouse gas inventories, report, Geneva, Switzerland. (Available at http://www.ipcc-nggip.iges.or.jp/public/gl/invs1.htm)

Intergovernmental Panel on Climate Change (IPCC) (2000), Good practice guidance and uncertainty management in national greenhouse gas inventories, report, NGGIP, Geneva, Switzerland.

Kaminski, T., P. J. Rayner, M. Heimann, and I. G. Enting (2001), On aggregation errors in atmospheric transport inversions, *J. Geophys. Res.*, *106*(D5), 4703–4715, doi:10.1029/2000JD900581.

Kirchgessner, D. A., S. D. Piccot, and A. Chada (1993), Estimation of methane emissions from a surface coal mine using open-path FTIR spectroscopy and modeling techniques, *Chemosphere*, *26*(1–4), 23–44, doi:10.1016/0045-6535(93)90410-7.

Kort, E. A., J. Eluszkiewicz, B. B. Stephens, J. B. Miller, C. Gerbig, T. Nehrkorn, B. C. Daube, J. O. Kaplan, S. Houweling, and S. C. Wofsy (2008), Emissions of CH_4 and N_2O over the United States and Canada based on a receptor-oriented modeling framework and COBRA-NA atmospheric observations, *Geophys. Res. Lett.*, *35*, L18808, doi:10.1029/2008GL034031.

Krol, M. C., S. Houweling, B. Bregman, M. van den Broek, A. Segers, P. van Velthoven, W. Peters, F. Dentener, and P. Bergamaschi (2005), The two-way nested global chemistry-transport zoom model TM5: Algorithm and applications, *Atmos. Chem. Phys.*, *5*, 417–432, doi:10.5194/acp-5-417-2005.

Krol, M. C., J. F. Meirink, P. Bergamaschi, J. E. Mak, D. Lowe, P. Jöckel, S. Houweling, and T. Röckmann (2008), What can ^{14}CO measurements tell us about OH?, Atmos, *Chem. Phys.*, *8*, 5033–5044, doi:10.5194/acp-8-5033-2008.

Lelieveld, J., S. Lechtenböhmer, S. S. Assonov, C. A. M. Brenninkmeijer, C. Dienst, M. Fischedick, and T. Hanke (2005), Greenhouse gases: Low methane leakage from gas pipelines, *Nature*, *434*, 841–842, doi:10.1038/434841a.

Levin, I., H. Glatzel-Mattheier, T. Marik, M. Cuntz, and M. Schmidt (1999), Verification of German methane emission inventories and their recent changes based on atmospheric observations, *J. Geophys. Res.*, *104*(D3), 3447–3456, doi:10.1029/1998JD100064.

Manning, A. J., D. B. Ryall, R. G. Derwent, P. G. Simmonds, and S. O'Doherty (2003), Estimating European emissions of ozone-depleting and greenhouse gases using observations and a modeling back-attribution technique, *J. Geophys. Res.*, *108*(D14), 4405, doi:10.1029/2002JD002312.

Matthews, E., I. Fung, and J. Lerner (1991), Methane emission from rice cultivation: Geographic and seasonal distribution of cultivated areas and emissions, *Global Biogeochem. Cycles*, *5*, 3–24, doi:10.1029/90GB02311.

Meirink, J. F., P. Bergamaschi, and M. Krol (2008), Four-dimensional variational data assimilation for inverse modelling of atmospheric methane emissions: Method and comparison with synthesis inversion, *Atmos. Chem. Phys.*, *8*, 6341–6353, doi:10.5194/acp-8-6341-2008.

Messager, C., M. Schmidt, M. Ramonet, P. Bousquet, P. Simmonds, A. Manning, V. Kazan, G. Spain, S. G. Jennings, and P. Ciais (2008), Ten years of CO_2, CH_4, CO and N_2O fluxes over western Europe inferred from atmospheric measurements at Mace Head, Ireland, *Atmos. Chem. Phys. Discuss.*, *8*, 1191–1237, doi:10.5194/acpd-8-1191-2008.

Prinn, R. G., et al. (2000), A history of chemically and radiatively important gases in air deduced from ALE/GAGE/AGAGE, *J. Geophys. Res.*, *105*(D14), 17,751–17,792, doi:10.1029/2000JD900141.

Rigby, M., et al. (2008), Renewed growth of atmospheric methane, *Geophys. Res. Lett.*, *35*, L22805, doi:10.1029/2008GL036037.

Rödenbeck, C., S. Houweling, M. Gloor, and M. Heimann (2003), CO_2 flux history 1982–2001 inferred from atmospheric data using a global inversion of atmospheric transport, *Atmos. Chem. Phys.*, *3*, 1919–1964, doi:10.5194/acp-3-1919-2003.

Schmidt, M., et al. (2006), RAMCES: The French Network of Atmospheric Greenhouse Gas Monitoring, *Rep. 168*, pp. 165–174, WMO, Geneva, Switzerland.

Shorter, J. H., et al. (1996), Methane emission measurements in urban areas in eastern Germany, *J. Atmos. Chem.*, *24*, 121–140, doi:10.1007/BF00162407.

Spivakovsky, C. M., et al. (2000), Three-dimensional climatological distribution of tropospheric OH: Update and evaluation, *J. Geophys. Res.*, *105*(D7), 8931–8980, doi:10.1029/1999JD901006.

Stephens, B. B., et al. (2007), Weak northern and strong tropical land carbon uptake from vertical profiles of atmospheric CO_2, *Science*, *316*, 1732–1735, doi:10.1126/science.1137004.

van der Maas, C. W. M., et al. (2009), Greenhouse gas emissions in the Netherlands 1990–2007, Neth. Environ. Assess. Agency, Bilthoven, Netherlands.

van der Werf, G. R., J. T. Randerson, G. J. Collatz, L. Giglio, P. S. Kasibhatla, A. F. Arellano Jr., S. C. Olsen, and E. S. Kasischke (2004), Continental-scale partitioning of fire emissions during the 1997 to 2001 El Niño/La Niña period, *Science*, *303*, 73–76, doi:10.1126/science.1090753.

Villani, M. G., P. Bergamaschi, M. Krol, J. F. Meirink, and F. Dentener (2010), Inverse modeling of European CH_4 emissions: Sensitivity to the observational network, *Atmos. Chem. Phys.*, *10*, 1249–1267, doi:10.5194/acp-10-1249-2010.

Wunch, D., P. O. Wennberg, G. C. Toon, G. Keppel-Aleks, and Y. G. Yavin (2009), Emissions of greenhouse gases from a North American megacity, *Geophys. Res. Lett.*, *36*, L15810, doi:10.1029/2009GL039825.

Zhao, C., A. E. Andrews, L. Bianco, J. Eluszkiewicz, A. Hirsch, C. MacDonald, T. Nehrkorn, and M. L. Fischer (2009), Atmospheric inverse estimates of methane emissions from Central California, *J. Geophys. Res.*, *114*, D16302, doi:10.1029/2008JD011671.

P. Bergamaschi, F. Dentener, S. Monni, and A. Segers, Institute for Environment and Sustainability, European Commission Joint Research Centre, I-21027 Ispra, Italy. (peter.bergamaschi@jrc.ec.europa.eu)

E. J. Dlugokencky, Global Monitoring Division, Earth System Research Laboratory, NOAA, Boulder, CO 80305, USA.

R. E. Fisher and E. G. Nisbet, Department of Earth Sciences, Royal Holloway, University of London, Egham TW20 0EX, UK.

M. Krol, SRON Netherlands Institute for Space Research, NL-3584 Utrecht, Netherlands.

F. Meinhardt, Umweltbundesamt, Messstelle Schauinsland, D-79199 Kirchzarten, Germany.

J. F. Meirink, Climate and Seismology Department, Royal Netherlands Meteorological Institute, NL-3732 GK De Bilt, Netherlands.

S. O'Doherty, School of Chemistry, University of Bristol, Bristol BS8 1TS, UK.

M. Ramonet, M. Schmidt, and C. Yver, Laboratoire des Sciences du Climat et de l'Environment, F-91198 Gif sur Yvette, France.

J. van Aardenne, Air and Climate Change Programme, European Environment Agency, DK-1050 Copenhagen, Denmark.

A. T. Vermeulen, Department of Biomass, Coal and Environment, Energy Research Centre of the Netherlands, NL-1755 ZG Petten, Netherlands.